Astron. Astrophys. 332, 449–458 (1998)

ASTRONOMY
AND
ASTROPHYSICS

ROSAT HRI observations of six early-type galaxies

Michael Dahlem[1] **and Norbert Stuhrmann**[2]

[1] ESTEC, Astrophysics Division, Space Science Department, Postbus 299, 2200 AG Noordwijk, The Netherlands
[2] Schwalbenweg 6, D-55765 Birkenfeld, Germany

Received 1 September 1997 / Accepted 20 November 1997

Abstract. High-resolution ROSAT HRI soft X-ray observations of four E/S0 galaxies were conducted by us. The data show no signs of Seyfert activity in the X-ray regime. The central emission peaks of the four galaxies, NGC 533, NGC 2832, NGC 4104 and NGC 6329, are associated with their cooling flows. The half intensity radii of the cooling flows range from 0.8 to 3.5 kpc. We find a trend (based up to now on only five objects) of the radio power of the cores in E/S0 galaxies to increase with the size and the accretion rates of their cooling flows.

In one galaxy, NGC 4921, no centrally peaked extended gaseous envelope was found, which is most likely due to the fact that it is not an E/S0 galaxy, but an early-type spiral.

NGC 2885, the sixth galaxy in our initial sample, shows signs of X-ray emission from an AGN. It has also been classified as a Sy-1 AGN by Bade et al. (1995). However, optical imaging suggests that this galaxy is probably not an E or S0 type system either, but rather an early-type spiral galaxy. Thus, in the context of accretion rate vs. galaxy type models of low-luminosity AGNs, the presence of an X-ray luminous Sy-1 nucleus in NGC 2885 is no surprise.

Key words: cooling flows – galaxies: elliptical and lenticular, cD – intergalactic medium – galaxies: nuclei – X-rays: galaxies

1. Introduction

Most early-type (elliptical and lenticular; E and S0) galaxies host in their centres active nuclei, which are detectable as radio cores. The radio activity is in most cases not associated with optical high-excitation (Seyfert) emission line characteristics (Owen et al. 1995). Phillips et al. (1986) stated that "the relative emission line strengths in virtually every case were indistinguishable from those of LINER nuclei". Most of the optical line emission comes from a centrally concentrated, low-mass ISM (Heckman et al. 1989; Macchetto et al. 1996). Only very few low-luminosity E/S0 galaxies show evidence for the existence of Seyfert nuclei in their centres. Optical spectroscopy of ESO 138 G1 (Alloin et al. 1992), e.g., revealed the presence of high-excitation Sy-2 emission lines and Howell et al. (1997) found recently that the Sy-1 galaxy US 3215 has a gE2 morphology.

Soft X-ray observations of E/S0 galaxies exhibit strong emission, consisting of two major morphological constituents: an extended low surface brightness envelope and a central emission peak. These are usually identified with the hot intergalactic gas in which these galaxies are embedded and cooling flows close to their centres. A confirmation of this interpretation comes from X-ray spectroscopy (e.g., Sarazin 1988).

Up to now, X-ray detectors either did not have sufficiently high angular resolution to study the centres of E/S0 galaxies in detail (e.g., Einstein IPC, ROSAT PSPC, ASCA), or did not have sufficient sensitivity (e.g., Einstein HRI). The ROSAT HRI, however, can spatially resolve the central few kpc in E/S0 galaxies with sufficient sensitivity for useful morphological investigations. This prompted us to use the HRI for a study of the central X-ray sources in six galaxies, including a search for possible X-ray emission from AGNs. These galaxies had been identified as the optical counterparts of bright X-ray sources in the course of the Hamburg Quasar Survey (Hagen et al. 1995).

2. Observations and data reduction

The galaxies observed by us with the ROSAT HRI are listed in Table 1, together with the observing times of the individual pointings and a few basic parameters. The total amount of time allocated for the current project was ca. 90 ks.

The data reduction was performed in the IRAF/PROS software package by NOAO and SAO. Since there are no indications of bad data due to high background, no further event selection than that by the ROSAT Standard Analysis Software System (SASS) was applied. From the event lists we created images by summing up 3×3 detector pixels, thus creating $1\farcs5$ image pixels. The background was determined in several source free regions of each image. Since we found no evidence for systematic background differences across the field of view, mean values of the levels measured in the source free regions were subtracted as constant offsets. The source free areas for the background determination were chosen to be distributed around the target

Send offprint requests to: M.Dahlem (mdahlem@astro.estec.esa.nl)

Table 1. ROSAT HRI observations

Galaxy Name	Morph. Type[1]	$\alpha, \delta(2000)$[1] [^{h} ^{m} ^{s} , $^\circ$ $'$ $''$]	Observing Date	Integration Time [ks]
NGC 533	E3:	01 25 31.2, +01 45 33	1994 Jan. 10	5.71
			1994 July 20	6.05
NGC 2832	E+2, cD	09 19 46.8, +33 44 59	1994 Apr. 22	15.27
NGC 2885	S0	09 27 18.5, +23 01 12	1994 Nov. 18	4.70
			1995 Apr. 25	3.77
NGC 4104	S0	12 06 38.2, +28 10 31	1993 June 10	1.79
NGC 4921	SB(rs)ab	13 01 26.1, +27 53 10	1994 June 25–July 07	17.77
NGC 6329	E	17 14 14.9, +43 41 03	1994 Apr. 06–08	15.70
			1994 Aug. 24	4.11[2]
			1994 Aug. 26	15.57

Notes to Table 1: 1) From NED; 2) Not used in data analysis.

Table 2. Summary of results

Galaxy	Count Rate [s^{-1}]	$N(H)^1_{Gal}$ [10^{20} cm^{-2}]	ECF^2 [10^{11} cts cm^2 erg^{-1}]	f_x(0.1–2.4 keV) [10^{-14} erg s^{-1} cm^{-2}]	D^3 [Mpc]	L_x(0.1–2.4 keV) [10^{40} erg s^{-1}]
NGC 533	0.0311 ± 0.0025[4]	2.95	0.16	117	73	75
NGC 2832	0.0164 ± 0.0011	1.21	0.18	82.6	95	89
NGC 4104	0.0133 ± 0.0034	1.81	0.17	71.2	113	108
NGC 4921	0.0039 ± 0.0005	0.85	0.19	18.7	77	13
NGC 6329	0.0164 ± 0.0012[4]	1.24	0.18	82.6	111	121

Notes to Table 2:
1) From Hartmann & Burton (1997).
2) Energy conversion factor for a 1 keV Raymond-Smith spectrum; from the ROSAT User's Manual (Briel et al. 1994).
3) Adopting $H_\circ$ = 75 km s^{-1} Mpc^{-1} and a virgocentric infall velocity of 300 km s^{-1}.
4) Mean over two observing runs.

galaxies randomly. Only in the case of NGC 4921 the emission of the nearby Coma cluster of galaxies was avoided by systematically measuring the background only eastward of the target. After this step, the images were divided by the net integration time (Table 1) in order to obtain count rates.

In those cases in which more than one pointing was performed in order to obtain the full amount of requested observing time, we added up the individual images before normalising them in order to increase the signal-to-noise ratios. The 1994 Aug. 08 data of NGC 6329 were not used because of the limited number of photons received from the galaxy and nearby sources and the resulting difficulties in determining the correct attitude solution compared to the other two runs.

In the final images the angular resolution of the ROSAT X-ray telescope, including pointing jitter degradation of the PSF, was measured by fitting gaussian profiles to the emission distribution of the brightest point sources and deconvolving these by the smoothing function that had been applied before. The resulting values were subsequently used to deconvolve the observed source profiles and thereby determine their true extent.

In three cases, NGC 533, NGC 4104 and NGC 4921, the alignment of the optical and X-ray images was achieved by determining the mean offset between both frames based on optical identifications of serendipitously detected X-ray sources in the field of view. For the different galaxies, 7 to 16 sources were used.

In the cases of NGC 2832 and NGC 2885 we could not find suitable X-ray sources in the field of view. In the NGC 6329 pointing, we were not able to reliably identify any optical counterpart of the 7 strong X-ray point sources in the field of view. Therefore, we had to *adopt* that the X-ray and optical centres of these three galaxies are aligned. This appears to be a sensible assumption, because the X-ray emission of all three is strongly peaked and – in NGC 2885 – time variable. The distribution of the surrounding diffuse emission in NGC 2832 and NGC 6329 is radial symmetric with respect to the location of the strong central source. The pointing offset corrections for all six galaxies lie in the range from $1''$ to $17''$.

We used the PROS task $imcnts$ to sum up the total number of photons received from all objects after background subtraction. In all cases, the integration was performed in a circular aperture with a radius of $30''$ around the optical centre of the galaxy (which, for all practical purposes, spatially coincides with the

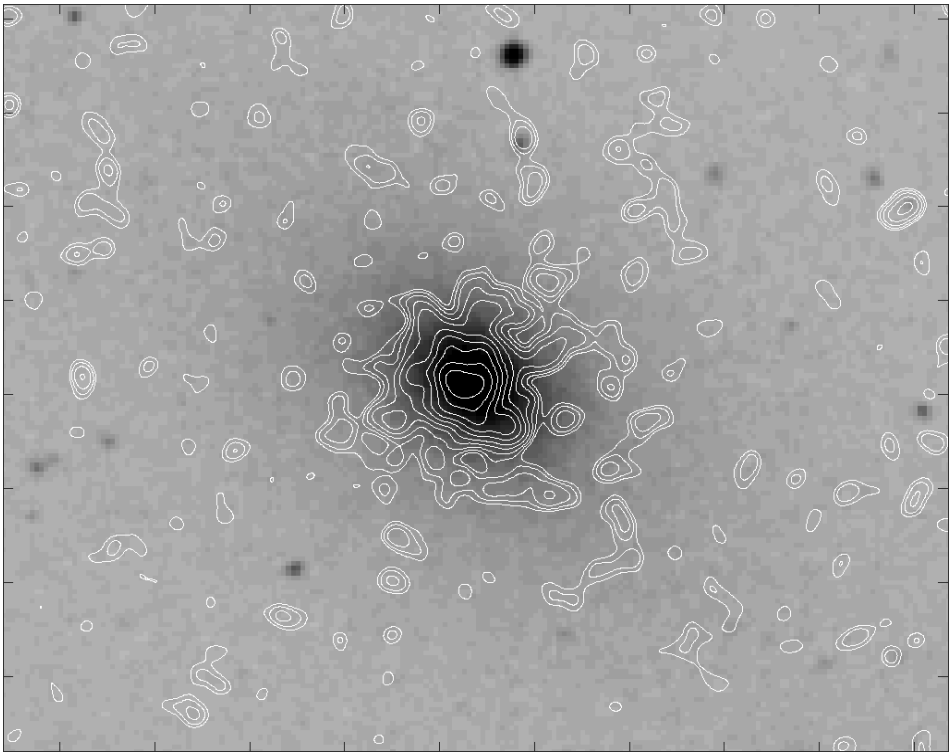

Fig. 1. Overlay of ROSAT HRI contours ontop of a DSS image of NGC 533. The X-ray image was smoothed to an angular resolution of $FWHM = 7''$. The contours start at $4.5\,10^{-6}$ cts pixel^{-1} s^{-1} (= $2\,\sigma$), increasing by factors of $\sqrt{2}$. The displayed field of view is $5' \times 4'$, centred on the nucleus of the galaxy.

centre of the X-ray emission for all six targets). The resulting count rates were used to calculate the source fluxes.

3. Results

The final HRI images of all six galaxies are shown in Figs. 1–6, overlaid on optical images from the Digitized Sky Survey (DSS). All X-ray images were smoothed to a resolution of $7''$. At the distances of the galaxies, this resolution corresponds to spatial scales of ca. 2.5 to 3.8 kpc. In all cases the displayed field of view is $5' \times 4'$. Using other lookup tables for the displays of the optical images, one could see that some of the galaxies are more extended than shown, but displaying them to their full extent would make it impossible to discern details in the highly concentrated X-ray emission distribution.

We investigated the morphological distribution of soft X-ray emission by fitting two-dimensional gaussians to the emission profiles. From these studies we obtained major axis position angles (*PA*s) and axial ratios (ellipticities, ϵ) for the X-ray emission distributions.

In order to quantify the extents of the central peaks, we measured the half intensity radii, $r_{\rm core}$, i.e. the *HWHM* of the X-ray emission distributions. Since the measured ellipticities are almost constant over the extent of the X-ray emission detected by the HRI and the average values are low, deviations from circular symmetry were neglected in the determination of $r_{\rm core}$, and the mean values were used. Note that this $r_{\rm core}$ is **not** that of the diffuse gaseous envelope (Mulchaey et al. 1996), but that of the central emission peak (i.e. the cooling flow).

3.1. NGC 533

Fig. 1 shows an emission distribution in the central part of NGC 533 with minor deviations from radial symmetry. The emission is clearly peaked in the central area, with some more low surface brightness emission around it. The ROSAT PSPC observations by Trinchieri et al. (1997; hereafter TFK97) indicate that this emission is part of a more extended envelope.

3.2. NGC 2832

NGC 2832, which is displayed in Fig. 2, shows a strong central emission peak, with some more diffuse emission around it. NGC 2831, ca. $25''$ southwest of NGC 2832, was also detected as a weak X-ray source. There is also a marginal detection on the nucleus of NGC 2830, which is the edge-on spiral ca. $80''$ southwest of NGC 2832. The Einstein IPC data by Fabbiano et al. (1992; hereafter FKT92) indicate the existence of a more extended gaseous envelope[1].

3.3. NGC 2885

NGC 2885 (Fig. 3) exhibits strong unresolved X-ray emission. A second source, which was serendipitously detected ca. $13''$ south of it, has no visible optical counterpart. Note that this is an image summed up from two observations. NGC 2885, without the confusing second source, is visible in Fig. 7. Both NGC 2885 and the southern source are highly variable in the X-ray regime.

[1] Note that in FKT92 NGC 2830 is mislabeled as NGC 2831 (which is the small elliptical galaxy closer to NGC 2832).

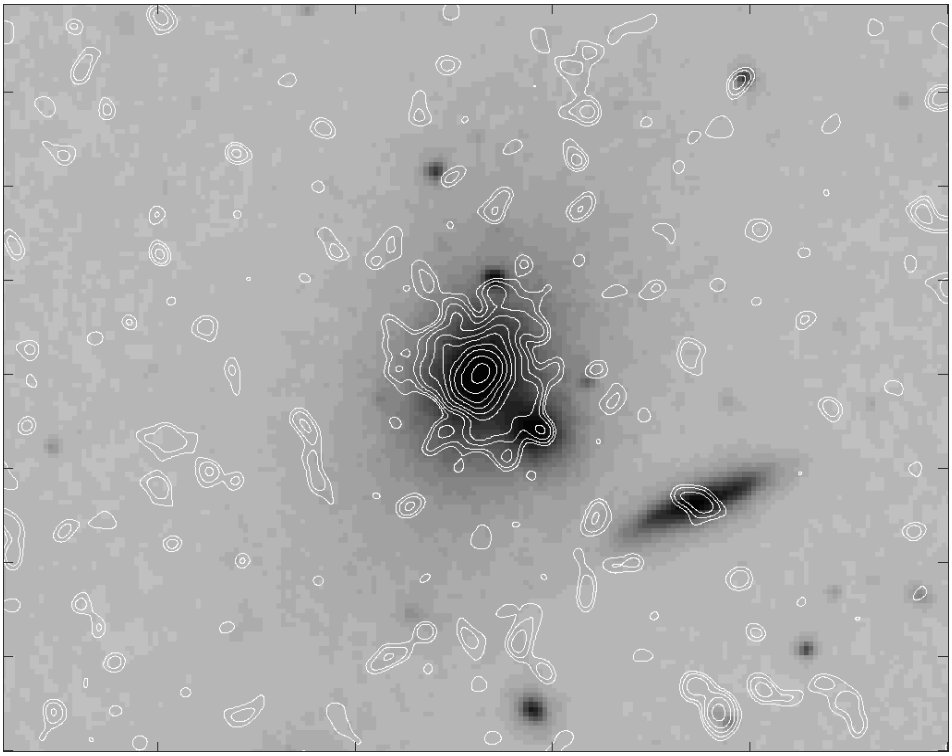

Fig. 2. Overlay of ROSAT HRI contours ontop of a DSS image of NGC 2832. The X-ray image was smoothed to an angular resolution of *FWHM* = 7″. The contours start at 3.9 10^{-6} cts pixel^{-1} s^{-1} (= 2 σ), increasing by factors of $\sqrt{2}$. The displayed field of view is 5′ × 4′, centred on the nucleus of the galaxy.

Strong X-ray variability on timescales of months was detected in NGC 2885 = RX J0927.3+2301 (Bade et al. 1995). The change in flux of the central source from the first observation to the second is a factor of 2.15. The variability of the bright unresolved central X-ray source indicates the existence of a Seyfert nucleus. Thus, we determined the X-ray flux, f_x, under the assumption of an α = 1 power law emission spectrum (attenuated only by Galactic foreground gas). α = 1 is close to the value determined by Bade et al. (1995) of $\alpha = 0.88 \pm 0.19$.

Both our observations show a source (or sources) that are considerably brighter than during the ROSAT All-sky Survey (RASS; Bade et al. 1995). At that time (the second half of 1990), the PSPC count rate of RX J09237+2301 was 0.2 cts s^{-1}. Comparing the PSPC energy conversion factor (ECF) listed by Briel et al. (1994), of 0.55 10^{11} cts cm^2 erg^{-1}, with that for the HRI, the PSPC count rate corresponds to an expected HRI count rate of 0.034 cts s^{-1}. On 1994, Nov. 18 we measured 0.24 cts s^{-1} with the HRI. Considering that the PSPC cannot resolve the two sources, we can also compare the expected HRI count rate at the time of the RASS with the combined HRI count rate of RX J09237+2300 and NGC 2885 in the 1995 Apr. 25 data of 0.353 cts s^{-1}. This means that the variability from the RASS to our observations exceeds factors of 7 and 10, respectively. The luminosity of NGC 2885 lies around 10^{43} erg s^{-1}, which is ca. 15–45 times higher than those of the central parts of the E/S0 galaxies listed in Table 2. Note that even this value of L_x is a lower limit because of the assumption of the absence of intrinsic X-ray absorption.

Optical imaging (DSS, see Fig. 3, and a B-band image by N. Bade) suggests that NGC 2885 is an early-type spiral galaxy, possibly of type Sa. The observed X-ray luminosity and variability confirm the identification of NGC 2885 as a Seyfert galaxy from optical spectroscopy (Bade et al. 1995). The galaxy's classification (NED; RC3) as an S0 galaxy is doubtful, however.

3.3.1. RX J0927.3+2300

According to the IAU naming convention we name the source south of NGC 2885, at the coordinates $\alpha, \delta(2000)$ = $09^h\ 27^m\ 18\overset{s}{.}6, +23^\circ\ 00'\ 57''$, RX J0927.3+2300. This source has no visible optical counterpart down to a limiting magnitude of order 20 mag (DSS) and in the optical images available to us, which suggests that it might be an optically faint background Seyfert nucleus or QSO.

As with NGC 2885, RX J0927.3+2300 is unresolved in the HRI image. At the time of the first observation it was not detected. We estimate an upper limit on its count rate during the first run of 0.002 cts s^{-1}, taking into account that there is some low surface brightness emission in the vicinity which increases the local "background" at the source position. During the second run, the count rate was 0.2414 cts s^{-1}. This leads to a minimum variability in the ROSAT band by a factor of 120 over a timescale of 5.5 months (see Table 3).

In Fig. 7 we display contour plots of the two HRI pointings plus a difference image with the central source in NGC 2885 subtracted. For this subtraction, the count rate in the first pointing was scaled to that of the second observing run. The difference image shows only the source RX J0927.3+2300 and some residual emission around the galaxy centre. The scaling factor

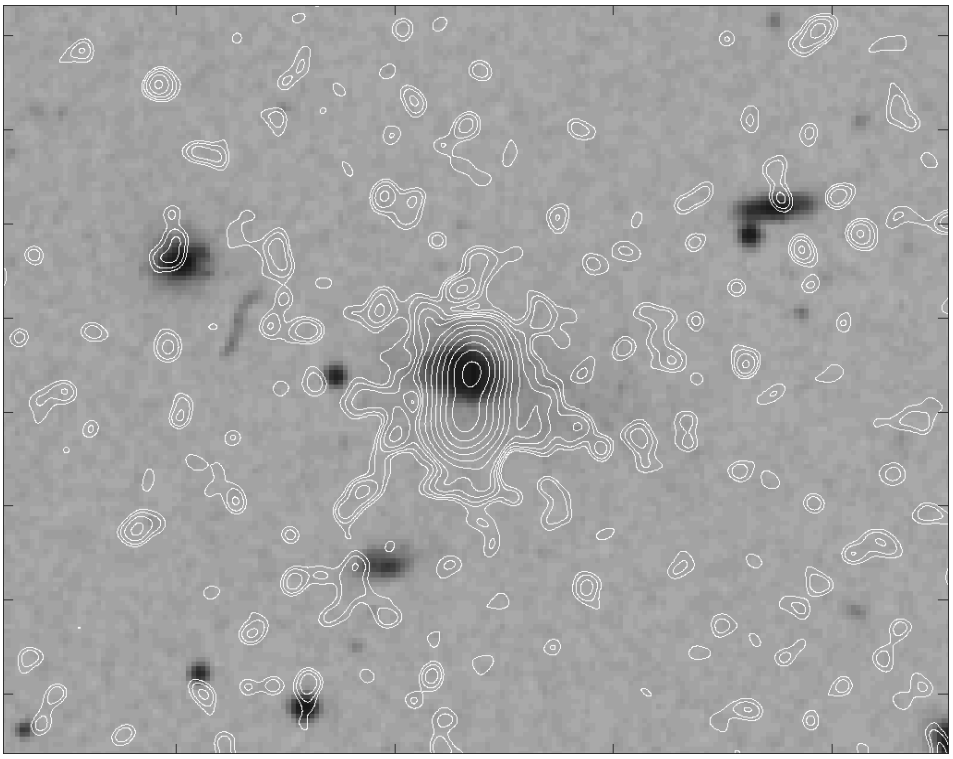

Fig. 3. Overlay of ROSAT HRI contours ontop of a DSS image of NGC 2885. The X-ray image was smoothed to an angular resolution of $FWHM = 7''$. The contours start at $4.9\,10^{-6}$ cts pixel^{-1} s^{-1} ($= 2\,\sigma$), increasing by factors of $\sqrt{2}$ up to the fifth contour ($= 8\,\sigma$). From there on, due to the high dynamic range of the image, the contours are separated by factors of 2. The displayed field of view is $5' \times 4'$, centred on the nucleus of the galaxy.

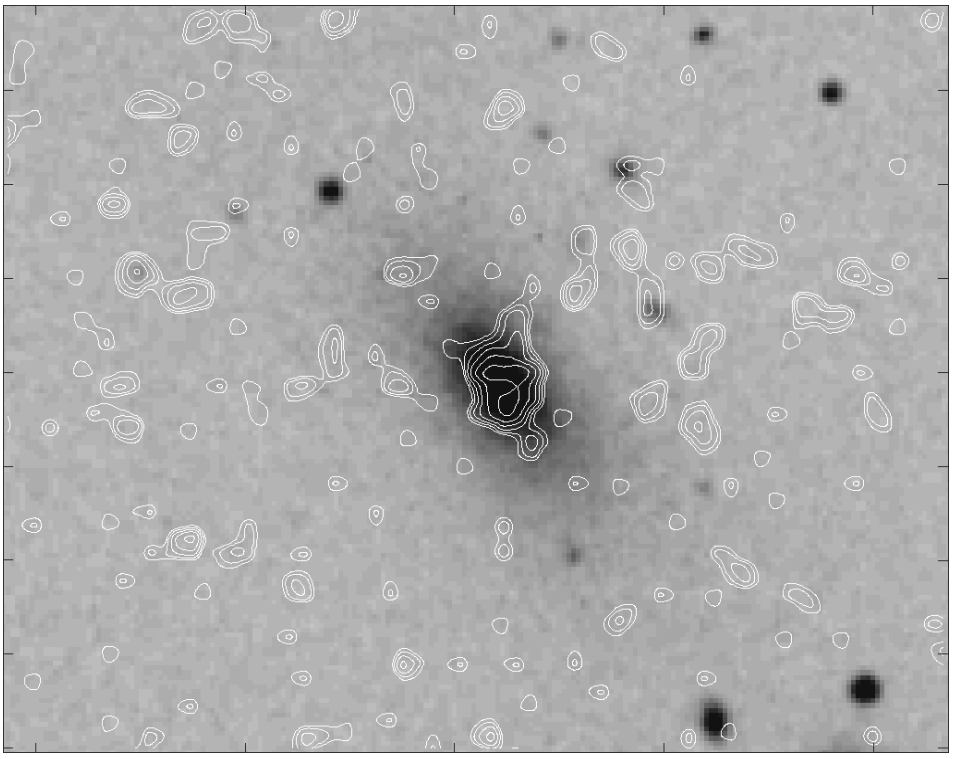

Fig. 4. Overlay of ROSAT HRI contours ontop of a DSS image of NGC 4104. The X-ray image was smoothed to an angular resolution of $FWHM = 7''$. The contours start at $1.0\,10^{-5}$ cts pixel^{-1} s^{-1} ($= 2\,\sigma$), increasing by factors of $\sqrt{2}$. The displayed field of view is $5' \times 4'$, centred on the nucleus of the galaxy.

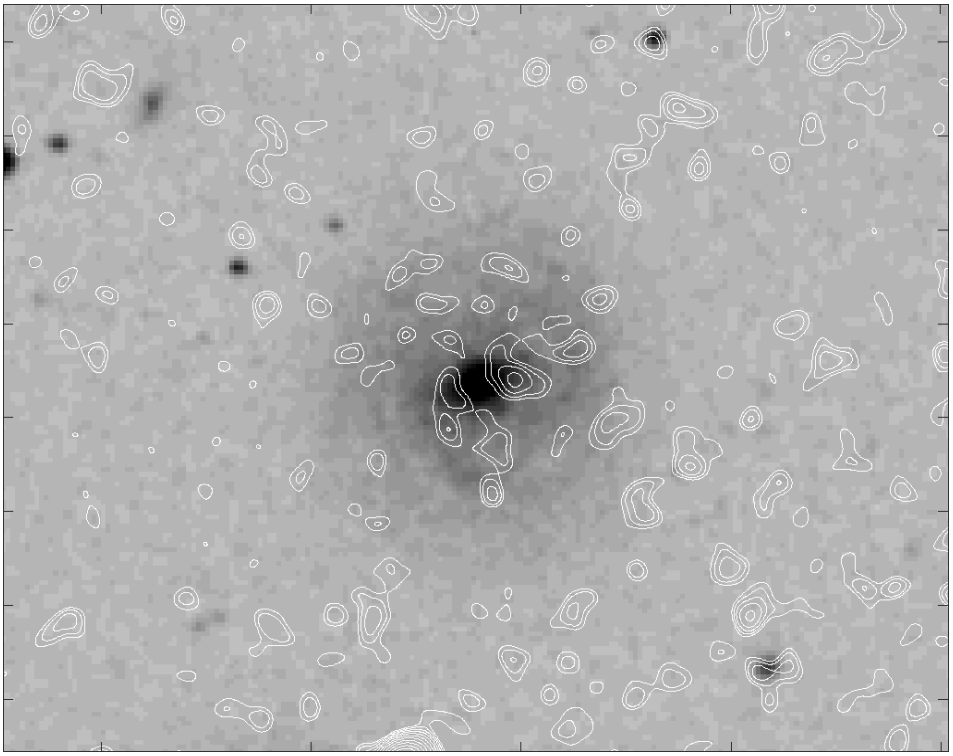

Fig. 5. Overlay of ROSAT HRI contours ontop of a DSS image of NGC 4921. The X-ray image was smoothed to an angular resolution of $FWHM = 7''$. The contours start at $3.6\,10^{-6}$ cts pixel^{-1} s^{-1} (= $2\,\sigma$), increasing by factors of $\sqrt{2}$. The displayed field of view is $5' \times 4'$, centred on the nucleus of the galaxy.

Table 3. Source variability of NGC 2885 and RX J0927.3+2300

Source Name	Obs. Date	Count Rate [s^{-1}]	f_x(0.1–2.4 keV)[1,2] [10^{-12} erg s^{-1} cm^{-2}]	L_x(0.1–2.4 keV)[3] [10^{40} erg s^{-1}]
NGC 2885	1994 Nov. 18	0.2392 ± 0.0074	25.7	3270
NGC 2885	1995 Apr. 25	0.1115 ± 0.0182	12.0	1525
RX J0927.3+2300	1994 Nov. 18	< 0.002	< 0.22	...
RX J0927.3+2300	1995 Apr. 25	0.2414 ± 0.0083	26.0	...

Notes to Table 3:
1) $N(\mathrm{H})_{\mathrm{Gal}} = 2.82\,10^{20}$ cm^{-2}; Hartmann & Burton (1997).
2) The energy conversion factor (ECF) for an $\alpha = 1$ power law spectrum, with $N(\mathrm{H})_{\mathrm{Gal}}$ as above, is $0.093\,10^{11}$ cts cm^2 erg^{-1} (Briel et al. 1994).
3) For $D = 103$ Mpc.

of 2.15 that was applied is a measure for the central source's variability within 5.5 months.

3.4. NGC 4104

The image of NGC 4104 in Fig. 4 reveals a pronounced concentration of X-ray emission in the central region. Note that the total number of source counts above the background is, due to the short integration time (Table 1), only 24. Earlier observations with the PSPC (Thiering & Dahlem 1998; hereafter TD98) exhibit a much wider emission distribution, of which the photons detected by the HRI represent the central peak.

3.5. NGC 4921

In NGC 4921 (Fig. 5) only little X-ray emission was detected. This emission is not concentrated at the centre of the galaxy (as would be usual for an E or S0 type system), but it is rather diffuse, with several weak emission maxima. This shallow emission distribution of NGC 4921 indicates that there is no pronounced central concentration of X-ray emitting gas (Fig. 5), implying the absence of a cooling flow. The optical image of NGC 4921 and its classification in the RC3 catalogue (de Vaucouleurs et al. 1991) indicate that it is an early-type spiral galaxy. Thus, it is not massive enough to retain a gravitationally heated hot gaseous halo. This is consistent with its low L_x. We will therefore exclude it from further investigations of E/S0 galaxies intended here.

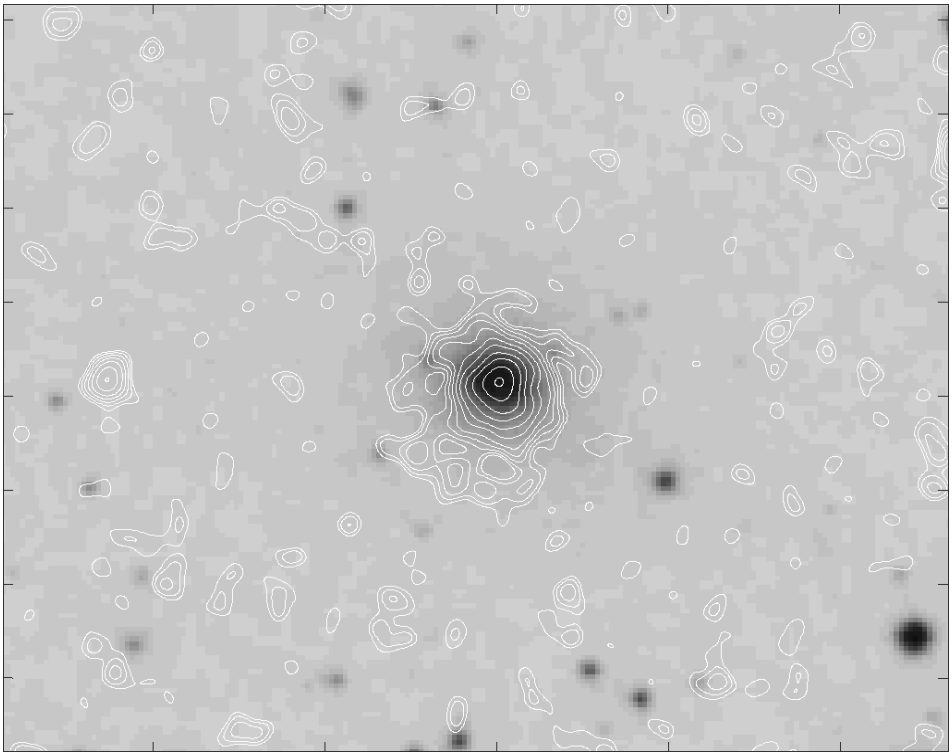

Fig. 6. Overlay of ROSAT HRI contours ontop of a DSS image of NGC 6329. The X-ray image was smoothed to an angular resolution of $FWHM = 7''$. The contours start at $2.8\,10^{-6}$ cts pixel^{-1} s^{-1} (= $2\,\sigma$), increasing by factors of $\sqrt{2}$. The displayed field of view is $5' \times 4'$, centred on the nucleus of the galaxy.

3.6. NGC 6329

The X-ray emission of NGC 6329, which is presented in Fig. 6, is concentrated at the centre, with some blobs of low surface brightness in its vicinity. Our PSPC observations (TD98) show that this peak is only the centre of a much more extended emission distribution and that the blobs are the brightest parts of an extended envelope.

3.7. Measured soft X-ray fluxes

In Table 2 we used the $N(\mathrm{H})_{\mathrm{Gal}}$ values of the Galactic foreground absorption and the distances, D, in columns 3 and 6 to convert the observed total count rates of five galaxies (mean values in cases where we have more than one pointing, summed over circular apertures of the central region with diameter $1'$) into fluxes, f_{x}, in the ROSAT band (0.1 to 2.4 keV) and soft X-ray luminosities, L_{x}, under the assumption of 1 keV Raymond-Smith (RS; Raymond & Smith 1977) plasmas with Solar abundances. The assumption of a 1 keV thermal plasma is justified by X-ray spectroscopy of E/S0 galaxies in the centres of groups and poor clusters, almost all of which (including NGC 533, NGC 4104 and NGC 6329; TFK97, TD98) have measured temperatures in the range from ca. 0.7 to 1.3 keV (see also Mulchaey et al. 1996; Matsumoto et al. 1997). The choice of aperture size (of $1'$) is justified by both our (DT98) results and those by TFK97, namely that the gas in galaxies at distances in the 50 – 100 Mpc range is cooler in the central $1'$ than further out (indicating that the aperture samples well the regions of the central cooling flows). The derived fluxes and luminosities are tabulated in columns 5 and 7 of Table 2. In the conversion of count rates to fluxes we applied a correction factor of 0.9 to the fluxes, because the ROSAT ECFs are given for 5×5 pixels, i.e., an area encircling only 90% of the energy, while we measure the total flux of the central sources in the target galaxies by using wider apertures.

In the data of the two E/S0 galaxies for which we have used two pointings each, the count rates of the two runs are identical to within 1–2%. Assuming perfect relative flux calibration of the two runs, this fraction of the measured total flux is an upper limit for possible contributions of variable sources.

4. Discussion

4.1. X-ray search for Seyfert nuclei in E/S0 galaxies

The galaxies with non-variable central emission peaks, namely NGC 533, NGC 2832, NGC 4104 and NGC 6329 (Figs. 1, 2, 4, and 6), are those that show indications in ROSAT PSPC and/or Einstein IPC observations of the presence of extended gaseous envelopes with central cooling flows. The peaks picked up by the ROSAT HRI are the "excess" emission from the cooling flows that is observed ontop of the shallower King profiles fitting the distributions of the extended gaseous halos. This extended emission is visible in our HRI data after degrading the angular resolution considerably (of order $20''$; not displayed). Thus, NGC 533, NGC 2832, NGC 4104 and NGC 6329 are the bona fide E/S0 systems in our sample. We find no signs for the presence of X-ray luminous Sy-1 nuclei in these four galaxies.

NGC 6329 has a strong central emission peak, but it is resolved at the resolution of the ROSAT HRI and therefore clearly associated with the hot gas.

Table 4. Extent of the central X-ray emission peaks

Galaxy	App. Ext.[1]	*PA* [°]	Ellipticity ϵ[2]	Ext. [″][3]	$r_{\rm core}$ [kpc][4]
NGC 533	14.9	25 ± 18	0.18 ± 0.09	14.6	2.6
NGC 2832	12.9	331 ± 4	0.15 ± 0.03	12.1	2.8
NGC 4104	4.3	4 ± 3	0.33 ± 0.08	2.8	0.8
NGC 6329	14.6	0 ± 15	0.13 ± 0.03	13.0	3.5

Notes to Table 4:
1) *FWHM* [″].
2) At a resolution of 7″; assumed to be 0 in the determination of the half light radius.
3) *FWHM*, assuming gaussian beam and emission distribution.
4) Calculated using the distances, D, listed in Table 2.

The central peak in NGC 4104 is not reliably resolved by the HRI, but its soft X-ray spectrum does not indicate any measurable contribution from a Seyfert nucleus (TD98). This galaxy also shows no evidence for optical high-excitation emission lines.

Neither NGC 533 nor NGC 6329, for which we have two datasets each, shows any sign of soft X-ray variability.

NGC 2885 does host a Sy-1 nucleus (Bade et al. 1995); however, it is most likely misclassified and therefore also no example for Seyfert activity of an E/S0 galaxy.

Thus, our soft X-ray data and those of other authors (TFK97; DT98; Mulchaey et al. 1996; Matsumoto et al. 1997; and many others) indicate that Seyfert activity (as opposed to nuclear radio activity) in E/S0 galaxies must be a rare phenomenon.

4.2. Extent of the central emission peaks

The central emission peaks in E/S0 galaxies, which are in most cases unresolved by the ROSAT PSPC or other energy-sensitive detectors, can be resolved into much more detail by the HRI. In Table 4 we list the beam-deconvolved half widths of the central maxima. Under the assumption that the observed emission is indeed associated with the central gas condensations, their extents give a measure of the core radii, $r_{\rm core}$. We find that these radii lie in the range from 0.8 kpc to 3.5 kpc.

NGC 6329 is the galaxy with the largest $r_{\rm core}$. Both NGC 533 and NGC 2832 have core radii of about 2.5 kpc (see Table 4), which lie in the middle of the range measured by us. The peak in NGC 4104 appears to be marginally resolved with the HRI, although the poor photon statistics makes this result unreliable, with an $r_{\rm core}$ of ca. 0.8 kpc. This is the smallest core radius found in the four galaxies studied here. The measured small extent of the central emission peak in NGC 4104 is compatible with the small cooling radius of the central cooling flow, $r_{\rm cool}$, calculated by us (TD98). NGC 4104 shows no signs of a significant power law continuum flux contribution from an AGN in our PSPC spectroscopy (TD98), corroborating that the emission comes from hot gas.

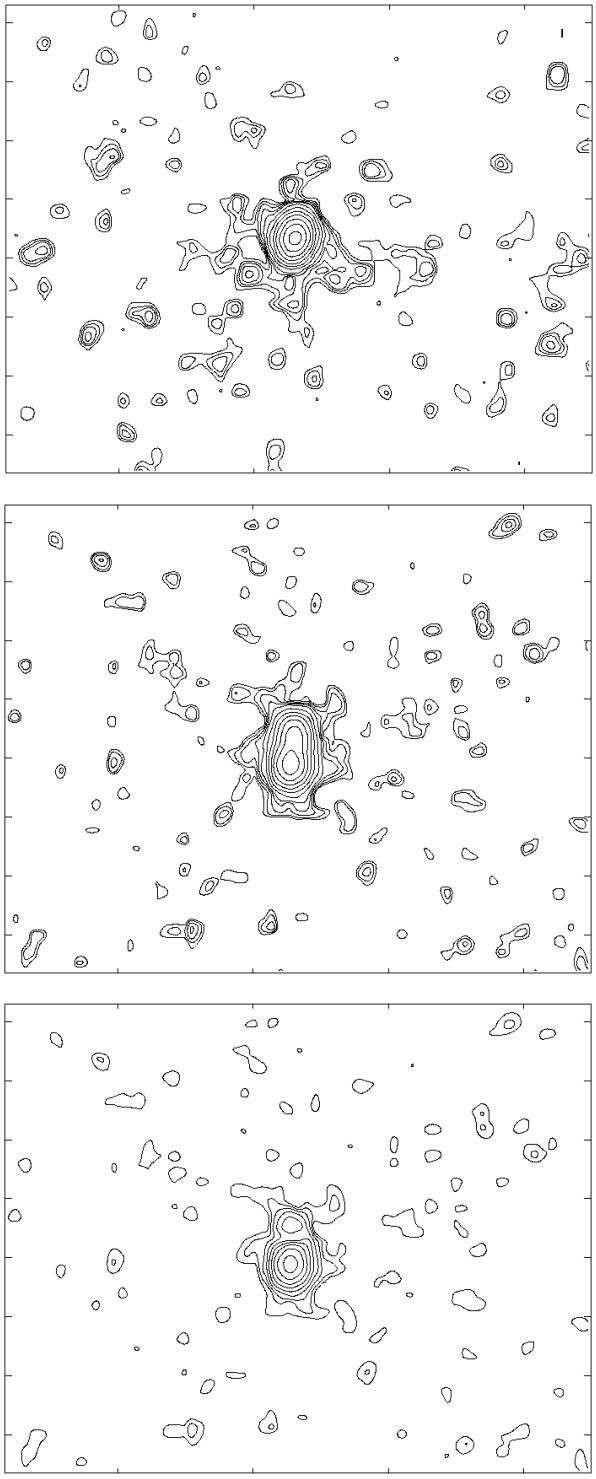

Fig. 7. 7″ *FWHM* HRI contour maps of NGC 2885. Upper panel: First observation (1994 Nov. 18). Middle panel: Second observing run (1995 Apr. 25). Lower panel: Difference image; see text for details. The contours of the two original images start at the $2\,\sigma$ level, increasing by factors of $\sqrt{2}$ up to the $8\,\sigma$ level, and by factors of 2 from there on in order to avoid contour crowding. The contours of the difference image are linearly spaced, starting at $2\,\sigma$, and increasing by $2\,\sigma$ each. The displayed field of view is again $5' \times 4'$, centred on the nucleus of the galaxy.

4.3. Comparison of the X-ray emission distribution with other wavebands

Comparing the fluxes measured from the HRI data and from existing PSPC observations, we find that ca. 10–25% of the total X-ray emission of the four E/S0 galaxies in our sample appear to come from the central few kpc (i.e. the areas dominated by emission from the cooling flows).

The soft X-ray light distributions of the four E/S0 galaxies presented here show no correlations with the optical emission distribution from the DSS. The X-ray emission profiles are close to circular even when the host galaxy is highly elliptical or lenticular in the optical. The measured position angles, *PA* (Table 4), do not correlate or anticorrelate with the optical position angles.

A comparison of our ROSAT results with radio data yields the following interesting trend: NGC 533, NGC 2832 and NGC 4104 are radio-weak (Calvani et al. 1989). We have PSPC data on 3 E/S0 galaxies: NGC 4104, NGC 6269 and NGC 6329. For NGC 4104 we deduced a low accretion rate (TD98). From the HRI image we determine a small $r_{\rm core}$ value for NGC 4104. Compared to NGC 4104, NGC 6329 has a higher $\dot{M}$ and a larger $r_{\rm core}$. This galaxy is a B3 (3rd Bologna catalogue) radio galaxy (e.g., Merighi et al. 1991). NGC 6269, for which we find the highest value of $\dot{M}$ (for the exact values see TD98), is a strong radio galaxy (e.g., Burns et al. 1981). The cooling radii that we derive from our PSPC data (TD98) also scale with $\dot{M}$ and the radio power of these systems.

The above might indicate a connection between the mass accretion rate, $\dot{M}$, of the cooling flows, their physical size, and the radio power of the cores in these galaxies, suggesting that the cooling flows are feeding the central engines. This is consistent with theories on black holes according to which the luminosity of the central engine depends on the mass supply rate from its environment and that Seyfert nuclei in spirals accrete near the Eddington limit, whereas radio cores in E/S0 galaxies accrete subcritically (see Blandford 1986). It is also consistent with the ideas of Bremer et al. (1997) on the onset of nuclear radio activity in the core of a central cluster galaxy with a cooling flow. However, we do not have enough information yet to make this a firm result. This is a subject to be investigated in more detail in the future, based either on ROSAT (HRI **and** PSPC) archival data of many more suitable objects or data from the next generation of X-ray satellites with good spatial and spectral resolution, such as, e.g., XMM or AXAF.

5. Conclusions

All bona fide E and S0 galaxies in our sample (NGC 533, NGC 2832, NGC 4104 and NGC 6329) have hot gaseous envelopes with central emission peaks in the soft X-ray regime. The peaks are associated with the central cooling flows. The measured half light radii, $r_{\rm core}$, of the cooling flows range from 0.8 to 3.5 kpc. None of them shows signs of X-ray luminous Sy-1 nuclei in the soft X-ray regime.

All our results are compatible with the scenario proposed, e.g., by Blandford (1986) and various others, according to which E/S0 galaxies host radio cores and spiral galaxies have Seyfert nuclei. The results from Sect. 4.3 are also consistent with the idea that the luminosities of active nuclei depend on the rate at which fuel is supplied. It will be important in the future to combine good spatial and spectral resolution in **one** dataset per galaxy to obtain homogeneous databases for more detailed studies of cooling flows in E/S0 galaxies, as well as groups and clusters dominated by such systems, and comparisons with their radio properties to study the effects of environmental influences on the evolution of the central galaxies and their nuclear activity.

Our data indicate that NGC 2885 and NGC 4921 are not E/S0 galaxyies. We confirm the results by Bade et al. (1995) with the detection of a highly variable central X-ray source in NGC 2885, which is associated with the optically identified Sy-1 nucleus. A second variable source is seen very close to NGC 2885, at a projected distance of only $13''$. No optical counterpart is known for this source.

Acknowledgements. N. Stuhrmann thanks B. Taylor for the kind hospitality received during a visit to ESTEC. We thank D. Hartmann for communicating the most up-to-date H I data. Thanks to N. Bade for providing us with an optical image of NGC 2885 and to the HQS group at Hamburger Sternwarte for their contributions to the optical identification of the X-ray sources. We thank the referee, Dr. N. Jackson, for useful comments. This research made use of the Digitized Sky Survey (DSS) which was produced at the Space Telescope Science Institute under U.S. Government grant NAG W-2166. The images of the survey are based on photographic data obtained using the Oschin Schmidt Telescope on Palomar Mountain and the UK Schmidt Telescope.

References

Alloin D., Bica E., Bonatto C., Prugniel P., 1992, A&A 266, 117
Bade N., Fink H. H., Engels D., et al., 1995, A&AS 110, 469
Blandford R. D., 1986, in IAU Symposium 87 on "Quasars", G. Swarup & V. K. Kapahi (eds.), p. 359
Bremer M. N., Fabian A. C., Crawford C. S., 1997, MNRAS 284, 213
Briel U., Aschenbach B., Hasinger G., et al., 1994, ROSAT Users' Handbook, MPE Garching
Burns J. O., White R. A., Hough D. H., 1981, AJ 86, 1
Calvani M., Fasano G., Franceschini A., 1989, AJ 97, 1319
Fabbiano G., Kim D.-W., Trinchieri G., 1992, ApJS 80, 645 (FKT92)
Hagen H.-J., Groote D., Engels D., Reimers, D., 1995, A&AS 111, 195
Hartmann D., Burton W. B., 1997, The Leiden-Dwingeloo Atlas of Galactic Neutral Hydrogen, Cambridge Univ. Press, Cambridge
Heckman T. M., Baum S. A., van Breugel W. J. M., & McCarthy P., 1989, ApJ 338, 48
Howell S. B., Pesce J. E., Condon J. J., Ciardullo R., Usher P. D. 1997, PASP 109, 1149
Macchetto F. D., Pastoriza M., Caon N., et al., 1996, A&AS 120, 463
Matsumoto H., Koyama K., Awaki H., et al., 1997, ApJ 482, 133
Merighi R., Basso L., Vigotti M., Lahulla J. F., Lopez-Arroyo M., 1991, A&AS 89, 225
Mulchaey J. S., Davis D. S., Mushotzky R. F., Burstein D. 1996, ApJ 456, 80
Owen F. N., Ledlow M. J., Keel W. C., 1995, AJ 109, 14
Phillips M. M., Jenkins C. R., Dopita M. A, Sadler E. M., Binette L., 1986, AJ 91, 1062
Raymond J. C., Smith B. H., 1977, ApJS 35, 419 (RS)

Sarazin C. L., 1988, "X-ray Emission of Clusters of Galaxies", Cambridge University Press, Cambridge
Thiering I., Dahlem M., 1998, A&A (subm.; TD98)
Trinchieri G., Fabbiano G., Kim D.-W., 1997, A&A 318, 361 (TFK)
de Vaucouleurs G., de Vaucouleurs A., Corwin H. G., et al., 1991, Third Reference Catalogue of Bright Galaxies, Springer-Verlag, New York, Berlin (RC3)

This article was processed by the author using Springer-Verlag LaTeX A&A style file *L-AA* version 3.